

Long-Lived Species Enhance Summertime Attribution of North American Ozone to Upwind Sources

Yixin Guo,^{†,§,‡,ⓑ} Junfeng Liu,^{*,†} Denise L. Mauzerall,^{§,ⓑ} Xiaoyuan Li,^{||} Larry W. Horowitz,[⊥] Wei Tao,[†] and Shu Tao^{†,ⓑ}

[†]Laboratory of Surface Processes, College of Urban and Environmental Sciences and [‡]School of Physics, Peking University, Beijing 100871, China

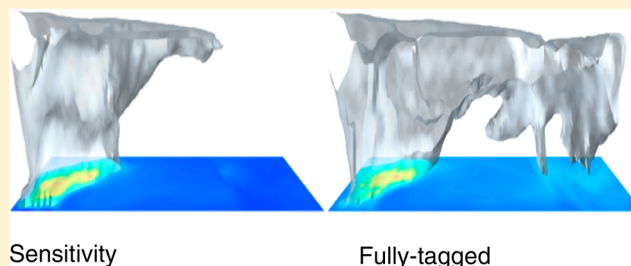
[§]Woodrow Wilson School of Public and International Affairs and ^{||}Department of Civil and Environmental Engineering, Princeton University, Princeton, New Jersey 08540, United States

[⊥]NOAA Geophysical Fluid Dynamics Laboratory, Princeton, New Jersey 08540, United States

Supporting Information

ABSTRACT: Ground-level ozone (O_3), harmful to most living things, is produced from both domestic and foreign emissions of anthropogenic precursors. Previous estimates of the linkage from distant sources rely on the sensitivity approach (i.e., modeling the change of ozone concentrations that result from modifying precursor emissions) as well as the tagging approach (i.e., tracking ozone produced from specific O_3 precursors emitted from one region). Here, for the first time, we tag all O_3 precursors (i.e., nitrogen oxides (NO_x), carbon monoxide (CO), and volatile organic compounds (VOCs))

from East Asia and explicitly track their physicochemical evolution without perturbing the nonlinear O_3 chemistry. We show that, even in summer, when intercontinental influence on ozone has typically been found to be weakest, nearly 3 parts per billion by volume (ppbv) seasonal average surface O_3 over North America can be attributed to East Asian anthropogenic emissions, compared with 0.7 ppbv using the sensitivity approach and 0.5 ppbv by tagging reactive nitrogen oxides. Considering the acute effects of O_3 exposure, approximately 670 cardiovascular and 300 respiratory premature mortalities within North America could be attributed to East Asia. CO and longer-lived VOCs, largely overlooked in previous studies, extend the influence of regional ozone precursors emissions and, thus, greatly enhance O_3 attribution to source region.



INTRODUCTION

Ground-level ozone (O_3) has adverse impacts on human health, crop yields, and ecosystems.^{1–5} In the United States, surface concentrations are regulated by the National Ambient Air Quality Standard (NAAQS) for O_3 that was tightened in 2015 from 75 to 70 nmol/mol (ppbv) over an 8 h average. As of 2015, 108.2 million people lived in counties with O_3 levels above the new NAAQS.⁶ In addition to U.S. anthropogenic sources that have been significantly mitigated in recent years (e.g., ~30% reduction for NO_x and CO during 2000–2010),⁷ background sources (e.g., natural or transboundary sources) contribute as much as 40–50 ppbv O_3 in spring and 25–40 ppbv in summer according to global model simulations.⁸

Ozone is a secondary pollutant, formed in the atmosphere by oxidation of volatile organic compounds (VOCs) and carbon monoxide (CO) in the presence of nitrogen oxides (NO_x). Sources of background O_3 include downward-mixing of stratospheric O_3 ,⁹ emissions from vegetation¹⁰ and wildfires,¹¹ and long-range transport from upwind regions, particularly East Asia.¹² During special meteorological conditions, trans-Pacific transport could enhance summertime U.S. surface ozone by 5–15 ppbv in the west and 2–5 ppbv in the east.^{12,13} Combined

satellite and model studies found that increased transpacific transport of O_3 has offset 43% of the 0.42 DU reductions in column-free tropospheric O_3 that could have occurred through domestic emission reductions between 2005 and 2010 over the western United States.¹⁴ Emissions of O_3 precursors have increased dramatically in East Asia due to a booming economy in which emissions of anthropogenic nitrogen oxides ($NO_x = NO + NO_2$) increased 25% between 2005 and 2010,¹⁵ carbon monoxide (CO) increased 25% between 2000 and 2010,¹⁶ and nonmethane volatile organic carbons (NMVOCs) increased 29% between 2001 and 2006.^{15,17} O_3 and its precursors (i.e., NO_x , CO, and NMVOCs) can be transported across the Pacific to the United States, during and after which O_3 formation takes place.¹⁸

O_3 precursor emissions and O_3 concentrations also alter the climate. The change of tropospheric O_3 level since the preindustrial times contributes to a radiative forcing of 0.40

Received: November 9, 2016

Revised: March 24, 2017

Accepted: March 28, 2017

Published: March 28, 2017

W/m².¹⁹ Tropospheric O₃ indirectly warms the climate through oxidizing forests, thus reducing carbon sink,²⁰ and indirectly cools the climate through affecting aerosol loading, especially sulfate.²¹

Attributing O₃ production to the source of its precursors is valuable for pollution management. Commonly used methods for quantifying the source-receptor linkages include sensitivity analysis and tagging techniques. Sensitivity analysis models the change of ozone concentrations that result from modifying precursor emissions and is widely used to demonstrate the potential air quality gains from a specific emission reduction measure.^{22–25} For example, the Hemispheric Transport of Air Pollution (HTAP) report found that decreasing East Asian anthropogenic precursor emissions by 20% would result in North American surface O₃ decreasing by 0.22 ppbv.²⁶ In addition, efforts made in the U.S. Environmental Protection Agency (EPA) emission-control programs substantially reduced local O₃ precursors emissions and lowered the 95th percentile ozone concentrations by 1–2 ppb per year during 1998–2003 summers.²⁷ Sensitivity analysis is a solution-originated method and is a powerful tool for scenario analysis. However, sensitivity analysis perturbs the nonlinear ozone chemistry (and local climate if coupled chemistry-climate model is used) and thus has difficulties in accurately attributing the current ozone abundance to individual emission sources.

The tagging technique is designed to attribute ozone produced within one region or from specific O₃ precursors. It adds regionally labeled artificial tracers for various species (including O₃ and O₃ precursors) and tracks the unperturbing current chemical or dynamical state of the system. It is a useful tool with which to identify sources and split responsibility for the adverse consequences of air pollution but is unable to conduct scenario analysis. There are several types of O₃-tagging approaches. For instance, O_x (O_x = O₃ + O + O(1D)) is tagged by the region in which it is produced. Thus, O_x production due to precursors both locally emitted and transported into the region is included, yet O_x produced outside the region due to precursors originating in the region are excluded.^{28–32} Alternatively, either NO_y (justified by the fact that, generally, NO_x-limited conditions for O₃ production are prevalent in most regions of the atmosphere) or VOCs (tracking VOC precursors and resulting peroxy and hydroperoxyl radical products)³³ originating in a region can be tagged, along with any O₃ formed by the reaction of the tagged precursors, regardless of where the formation occurs.^{34,35} In some studies, individual O₃ precursors are tagged, and O₃ production is assigned entirely to NO_x (VOCs) if it is regarded to happen in the NO_x-limited (VOCs-limited) regime.^{36,37}

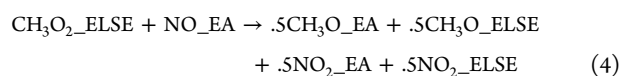
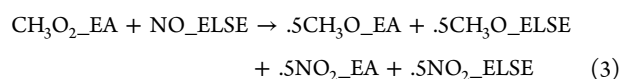
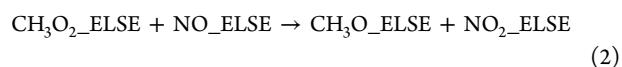
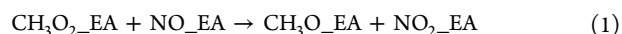
The above-mentioned pioneer modeling works have significantly improved our understanding of the roles of specific ozone precursors in ozone pollution formulations. To attribute O₃ pollution to all O₃ precursors in a more-coherent way, we develop a fully-tagged mechanism and apply it to trace the trans-Pacific influence (i.e., attributing the North American (NA) surface O₃ concentrations to all East Asian anthropogenic emissions (EA_AE)). Our mechanism transports tagged tracers of O₃ precursors (NO_y, CO, and VOCs) from a source and their oxidation products (e.g., NO_y, RO₂, RO, and HO₂) globally from source region to downwind receptor regions. When O₃ precursors from this source interact with precursors from other sources, half of the resulting species is attributed to each source. Compared with other O₃ source attribution mechanisms, this approach permits a complete and coherent

accounting of the impact of one region's emissions on all regions outside the source region through complex chain radical reactions of O₃ chemistry. We also conduct similar simulations using sensitivity analysis and NO_y-tagging approaches and then differentiate the inherent meaning of the results from the three techniques. All simulations are performed for the year 2000 using the global atmospheric chemistry transport model, the Model for Ozone and Related Chemical Tracers (MOZART-4) (see the [Materials and Methods](#) section).

■ MATERIALS AND METHODS

Sensitivity and NO_y-Tagging Methods. The sensitivity analysis is conducted with two parallel simulations with identical meteorological input: one with the standard emission inventory and one with all East Asian anthropogenic emissions (EA_AE) turned off. The difference in O₃ concentrations between the two simulations is taken as the contribution of EA_AE. The NO_y-tagging approach is conducted with multiple artificial tagged tracers and reactions added to the MOZART-4 photochemistry mechanism, representing East Asian anthropogenic NO_x emissions and their transformation within the NO_y family (e.g., PAN, HNO₃, and organic nitrates). The artificial tagged tracers are deposited at the same deposition rate as their corresponding real species; the tagged reactions exhibit the same reaction rate constants as the nontagged species. Descriptions of the tagged mechanism, as well as its implementation into MOZART-4 and CAM-Chem, can be found in Emmons et al.³⁴ The results from the sensitivity analysis and NO_y-tagging approaches in this study are consistent with previous analyses (see [Table S1](#)).^{26,35}

Fully-Tagged Method. The fully-tagged method adds two sets of artificial tracers to separately track all emissions and their consequent evolutions from East Asian anthropogenic sources (labeled as EA) and from other sources (labeled as ELSE). The standard MOZART-4 chemistry includes 85 gas-phase species and 196 reactions. Except for CO₂, H₂O, CH₄, H₂, N₂O, O₂, and N₂ (i.e., fixed or constant species), basically every species is assigned two additional tracers (EA and ELSE). These tagged species experience the same physical (transport and deposition) and chemical processes as the corresponding nontagged species but will not consume or generate any nontagged species. The rules for reactions of two tagged species are described by reactions 1–4). When both reactants are labeled as EA (or ELSE), all products are labeled as EA (or ELSE; see reactions 1 and 2). If one reactant is labeled as EA and the other is ELSE, we label half the amount of each product as EA and half as ELSE (see reactions 3 and 4). For unimolecular reactions (e.g., some photolysis ones), the labels of all products are identical to the reactant.



Reactions 3 and 4 implement an equal contribution rule to label products. This assumption originates from the classic chemical

kinetics theories (e.g., the collision theory, the transition-state theory, etc.) that explain how chemical reactions happen.³⁸ These theories all indicate the fact that a two-body reaction simultaneously involves the participation of two reactant molecules; thus, the role of one reactant is not superior to the other.³⁸ For example, when CH₃O₂ reacts with NO (see Figure 1), each reactant contributes an unpaired electron to

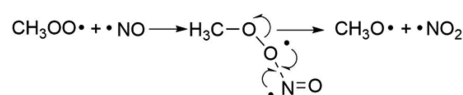


Figure 1. Arrow-pushing plot for the reaction between CH₃O₂ and NO. The single-sided arrowheads indicate transfer of electron from one bond to another.

form a chemical bond. The breaking of old bond and formation of new bond happen simultaneously. Lacking either reactant, the reaction will not happen. Therefore, the fully-tagged method interprets that all products are equally contributed by both reactants.

With the above rules, the fully-tagged mechanism adds 156 tagged tracers and 692 tagged reactions to the standard MOZART-4 chemistry mechanism. Some examples showing how we tag species and reactions are given in Tables S2–S4. For reactions involving CH₄, special treatment is used (details are given in the Supporting Information and Table S5). Results of the fully-tagged method are checked following Emmons et al.³⁴ The sum of O₃ from two individual sources (O₃_EA and O₃_ELSE) agrees well with the original untagged O₃ within 0.25% for every month in 2000 (see Figure S1).

Model Description and Configuration. We utilize the Model for Ozone and Related Tracers version 4 (MOZART-4) to simulate O₃ production and transport within the troposphere. MOZART-4 is particularly suited for studies of tropospheric chemistry. A detailed model description and a full model evaluation can be found in Emmons et al.³⁹

In this study, MOZART-4 is driven by NCEP–NCAR reanalysis meteorological fields with a horizontal resolution of 1.9° × 1.9° and a vertical resolution of 28 sigma vertical levels (Table S6) from the surface to about 2.7 hPa. The majority of anthropogenic emissions as well as all biogenic emissions are from Precursors of Ozone and Their Effects in Troposphere (POET) database,^{40,41} except for fossil fuel and biofuel combustion emissions, which are from the Emission Database for Global Atmospheric Research (EDGAR-3). The extra forcing and NO production from lightning are included.⁴² We simulate the 1999–2000 period and analyze results for the year 2000.

The model results have been extensively validated against several sets of global observations including the NOAA GMD (Global Monitoring Division) network, MOPITT (Measurement of Pollution in the Troposphere) CO, ozonesondes, and Moderate Resolution Imaging Spectroradiometer (MODIS) aerosol optical depth measurements, and the results show that MOZART-4 can well-reproduce tropospheric chemical composition and is suitable for tropospheric investigations on the regional to global scale.³⁹ Here, we compiled additional source of observations from the Acid Deposition Monitoring Network in East Asia (EANET) and validate the model results over East Asia for the year 2000.⁴³ The model reproduces relatively well the absolute concentration and seasonal variability of tropospheric O₃, even though the model slightly overestimates

summertime surface ozone concentrations for the Yonagunijima, Ryori, Ogasawara, Sado-seki, Happo, and Oki sites, and underestimate springtime surface ozone concentrations for the Tappi, Sado-seki, Happo, Oki, and Hedo sites (Figure S2).

These discrepancies are consistent with those found in Emmons et al.³⁹ and are partially caused by the coarse model resolution.³⁹ For example, pollution plumes in global models are typically diluted and insufficiently lofted to higher altitudes where they could have undergone more efficient transport in stronger winds.⁴⁴ In high-resolution models, the response of O₃ to emission perturbations was found to be 50% lower than in coarse-resolution models. In addition, underestimation of NO_x titration due to low resolution has also been found responsible for differences in surface O₃ in MOZART-4 compared with observations over China.⁴⁵ Besides model resolution, uncertainties in emission inventories may also contribute to model discrepancies (global inventories, e.g., POET, are usually compiled with less details in the timing and position of different emission activities than the EPA reported U.S. inventories, which have been used to support regulatory programs^{46,16,47}).

We apply sensitivity analysis, NO_y-tagging, and fully-tagged methods in MOZART-4 to characterize the trans-Pacific influence of East Asian anthropogenic emissions to North American surface O₃. The definition of East Asia (EA: 15–50° N and 95–160° E) and North America (NA: 15–55° N and 60–125° W) follows the definition in Fiore et al.²⁵ (see Figure S3).

Health Impact of O₃. We quantify the number of premature mortalities (unit: deaths) over North America that is associated with surface O₃ exposure attributable to EA_AE as eq 5:

$$\Delta\text{mortality} = \text{Pop} \cdot \text{Mb} \cdot (1 - \exp^{-\beta\Delta C}) \quad (5)$$

where Pop is population, Mb is the baseline mortality rate, ΔC is the amount of O₃ concentrations related to EA_AE by each mechanism, and β is concentration–response factor adopted from the time-series study, describing the acute effect of O₃ exposure on respiratory and cardiovascular mortality.³ For all age groups in NA, a 10 ppbv increase of 24-h averaged hourly O₃ is associated with an increased risk of respiratory and cardiovascular mortality of 0.65% and 0.85%, respectively.³ Current epidemiological studies do not reveal a clear O₃ concentration threshold under which no damage occurs. Previous studies have used no threshold and thresholds of 25 ppbv⁴⁸ and 35 ppbv.^{49,26} Here, we conduct the O₃ mortality calculation, assuming no threshold and a threshold of 25 ppbv.

We apply the equation above to every model grid within NA on a monthly basis and sum them up to get annual estimation, as was done in Anenberg et al.⁴⁹ Baseline monthly mortality rates of respiratory and cardiovascular diseases for the year 2000 are from National Center for Health Statistics and the Centers for Disease Control and Prevention.⁵⁰ The global population data is obtained from the Center for International Earth Science Information Network (CIESIN).⁵¹

RESULTS AND DISCUSSION

We find a substantially larger annual influence from East Asian anthropogenic emissions (EA_AE) to North American surface O₃ using the fully-tagged method (2.75 ppbv) than either the sensitivity analysis (1.11 ppbv) or by tagging NO_y alone (1.04 ppbv) (Table S1). All three methods find maximum seasonal transport in spring (1.65, 1.62, and 3.1 ppbv for sensitivity

approaches, NO_y-tagging, and fully-tagged methods, respectively) and relatively moderate transport in winter and fall (Figure 2). However, summertime fully-tagged transport is four

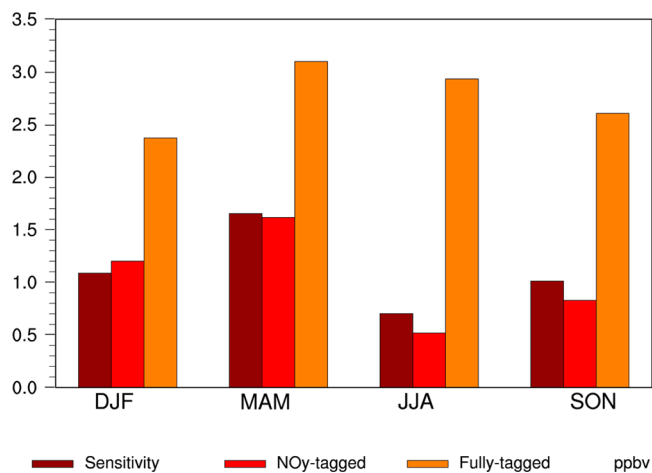


Figure 2. Seasonal average contribution of EA anthropogenic emissions to NA surface O₃ (ppbv) in 2000 using a sensitivity analysis (i.e., response of NA surface O₃ to the removal of East Asian anthropogenic emissions; brown), NO_y-tagging (i.e., tagging of all reactive nitrogen species and O_x; red) and fully-tagged (i.e., tagging of O_x and all O₃ precursors, including CO, VOCs, and NO_x; orange) approaches. EA is defined as 15–50° N and 95–160° E. NA is defined as 15–55° N and 60–125° W.

to nearly six times larger than transport found using the sensitivity and NO_y-tagging approaches (2.9, 0.7, and 0.5 ppbv, respectively). This result implies there may be larger EA influence during individual transport events when hourly or the MAD8 metric is used (will be evaluated in detail in our follow-up studies). Correspondingly, the annual minimum season of transport becomes winter in the fully-tagged approach and no longer summer, as in the NO_y-tagging and sensitivity approaches.

In summer, the fully-tagged mechanism captures the strong interactions of East Asian anthropogenic emissions with domestic NA emissions and thus obtains the largest O₃ contribution within the NA boundary layer. Surface winds over the Pacific are dominated by a high-pressure system, which favors Asian outflow north of 45° N but generally blocks eastward transport over the subtropical Pacific. Even so, all mechanisms show East Asian emissions impact O₃ levels near the edge of tropical easterlies and over the western United States in summer (Figure 3). This occurs partially because summertime transport goes through the free troposphere followed by descent in a high-pressure system near the west coast of NA. Figure S4 shows rapid East Asian O₃ production over the EA continent due to active photochemistry. High levels of East Asian O₃ and O₃ precursors are then deeply convected and exported across the Pacific (Figure S4). When the plume descends and interacts with local pollutants over North America, the fully-tagged approach generates substantially more East Asian O₃, both in the boundary layer (2–3

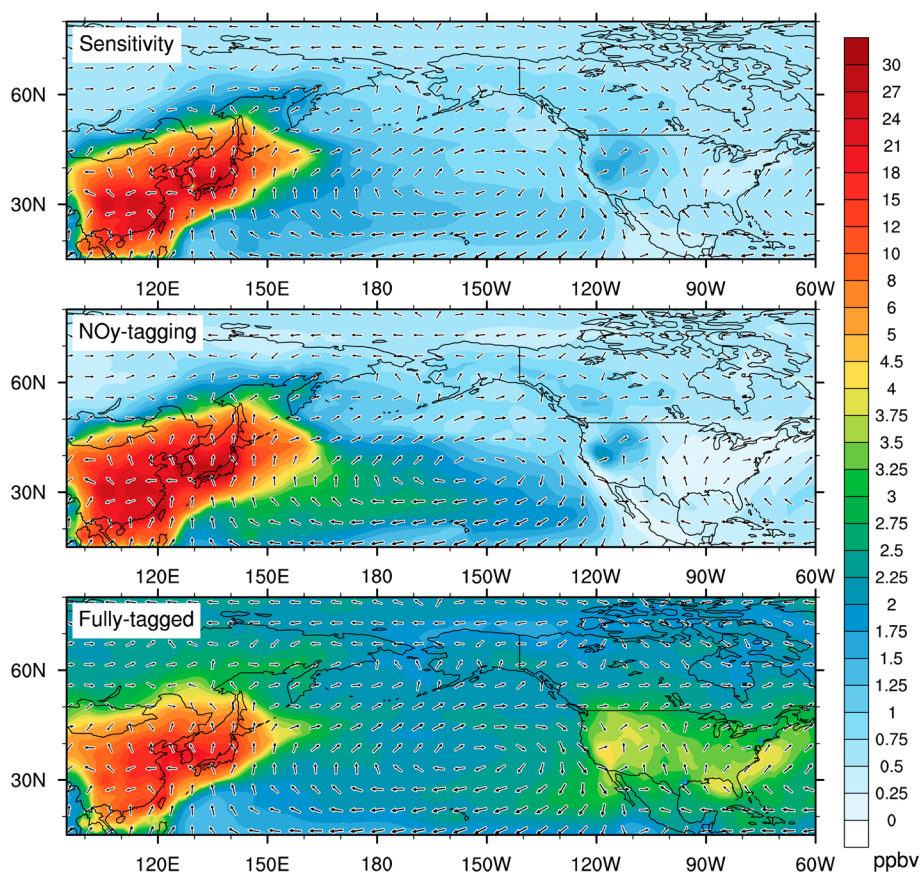


Figure 3. Simulated distribution of summertime (JJA) surface ozone (ppbv) contributed by EA anthropogenic emissions obtained using a sensitivity analysis (removal of East Asian anthropogenic emissions (EA_AE), top), NO_y-tagging (tagging of EA_AE of NO_x, middle), and fully-tagged (tagging of all EA_AE of O₃ precursors including CO, VOCs, and NO_x, bottom) approaches. Arrows indicate near-surface wind velocity (m·sec⁻¹).

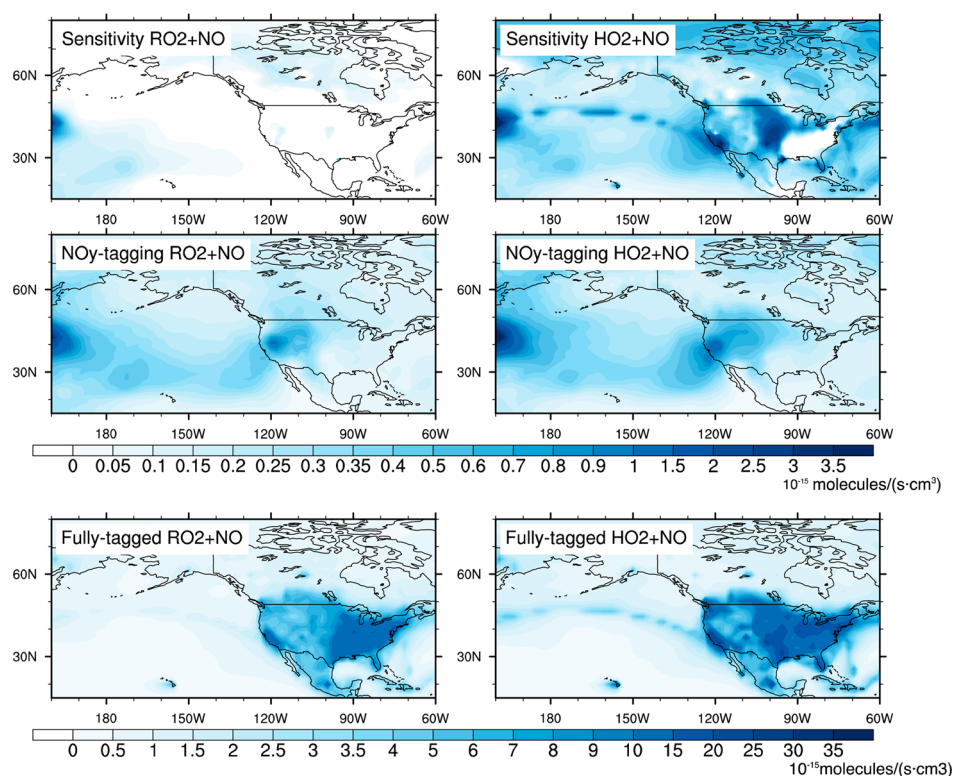


Figure 4. Simulated key O_x production pathways, i.e., the production rate in the summer (JJA) NO_2 (10^{-15} molecules/(s · cm³)) through the reaction $RO_2 + NO \rightarrow RO + NO_2$ (left) and $HO_2 + NO \rightarrow OH + NO_2$ (right) within the boundary layer (between surface and 800 hPa) over the Pacific and North America contributed by East Asia anthropogenic emissions, obtained using a sensitivity analysis (removal of East Asian anthropogenic emissions (EA_AE), top), NO_y -tagging (tagging of EA_AE of NO_x , middle), and fully-tagged (tagging of all EA_AE of O_3 precursors including CO, VOCs, and NO_x , bottom) approaches.

ppbv; Figures 3 and S4) and in the free troposphere (4–6 ppbv; Figure S4) than other mechanisms.

Although both the fully-tagged and NO_y -tagging mechanisms assign East Asian O_3 based on reactions of tagged East Asian NO_x , they determine the abundance of East Asian NO_x quite differently. In the NO_y -tagging mechanism, the East Asian NO_x is either directly emitted or recycled from other reactive nitrogen species (NO_y). NO_x itself and most reservoir species, except for PAN, typically have short lifetimes and are thus largely depleted before reaching the western United States. We thus examine the major pathways of East Asian NO_x production (thus EA O_3 production), i.e., NO to NO_2 conversion by RO_2 and HO_2 . As shown in Figure 4, the NO_y -tagging method demonstrates moderate East Asian O_3 production over North America within the boundary layer, especially in the east, during the summer (JJA). When averaged over the entire NA, the conversion rate of the tagged NO to tagged NO_2 (leading to tagged O_3 production) is 1.8×10^{-16} molecules/(s·cm³) by RO_2 and 2.3×10^{-16} molecules/(s·cm³) by HO_2 (Figure 4 and Table S7). Reaction amounts of other chemical pathways that are less important for O_3 and NO_2 concentrations (Figure S5) are provided in Table S7.

In contrast, the fully-tagged mechanism tracks the evolution of East Asian NO_x based on a reservoir of all reactive species. The fully-tagged procedure tags East Asian anthropogenic emissions of CO and VOCs in addition to NO_x and follows them through the formation of NO_y , RO_x , HO_x , etc. When East Asian outflow meets the U.S. air mass, longer-lived species (e.g., CO and certain VOCs species such as butane, propane, methanol, acetylene, etc.^{52,53}) originating in EA react with NO

from other sources, forming tagged East Asian shorter-lived species (NO_2 and RO) present at half the quantity as the resulting products. Furthermore, because NO_y , HO_x , and RO_x species are tagged, the source influence will persist until the tagged species are physically removed by dry–wet deposition or chemically converted to stable species (e.g., CO_2 , H_2O , etc.). This significantly reduces the rate of depletion of the tagged tracers and greatly enhances the abundance of East Asian NO_2 and, thus, East Asian O_3 in the U.S. boundary layer, evidenced by the large production rates of East Asian NO_2 from the tagged reaction of NO and RO_2 (4.5×10^{-15} molecules/(s·cm³) and the tagged reaction of NO and HO_2 (6.2×10^{-15} molecules/(s·cm³) (Figure 4 and Table S7). Previous studies indicated little baseline ozone (i.e., ozone influenced by sources other than local anthropogenic ones) impacts the surface of the eastern U.S.⁵⁴ The fully-tagged method highlights that the eastern United States experiences intensive EA source impact as large as 3–4 ppbv (Figure 3), with the secondary production of O_3 attributable to EA (Figures 4 and S6) as a dominant driver. There have been established studies of how high-elevation sites over the western United States are susceptible to intercontinental transport⁵⁵ and stratospheric intrusion,⁵⁶ while additional studies examining the extent and mechanism of the EA impacts over the eastern United States through chemistry, entrainment, etc., are needed. We have also conducted fully-tagged simulations that tag a portion of EA_AE, thus attributing NA O_3 to EA_AE NO_x and EA_AE VOCs plus CO, respectively. The larger attribution is via long-lived EA_CO plus EA_VOCs (around 2.5 ppbv), and the impact

from EA_NO_x is relatively smaller (around 0.5 ppbv) (Figure S7).

Unlike the tagging approaches, the sensitivity method compares the difference in O₃ simulated in two states of the atmosphere. Within the NA boundary layer, removing East Asian emissions increases the rate of transformation from NO to NO₂ through RO₂ by $2.8 \times 10^{-16}/(\text{s}\cdot\text{cm}^3)$ and decreases transformation from NO to NO₂ through HO₂ by $5 \times 10^{-16}/(\text{s}\cdot\text{cm}^3)$ (Figure 4 and Table S7). The difference of O₃ between a perturbed and a standard simulation can be approximately attributed to three sources: (1) O₃ produced by the enhanced EA precursors, (2) O₃ jointly produced by the enhanced EA and ELSE precursors, and (3) the changes in O₃ production by ELSE precursors due to the presence of EA_AE. The first two sources are partially offset by the third one because the presence of EA_AE not only decreases the O₃ production efficiency of ELSE NO_x and VOCs but also depresses the participation of ELSE CO and VOCs involved in the photochemical chain reactions.

All methods show that spring is the season with the strongest East Asian influence on NA surface O₃ levels (Figures 2 and S8). This springtime maximum is a result of several processes. First, rapid transport, assisted by frequent passage of cold front systems, increases the likelihood of short-lived species crossing the Pacific. Second, transport at midtroposphere and near surface enables a larger influence on surface O₃ concentrations (Figure S9). Third, although photochemistry is generally less active in spring than summer (for example, conversion rates of EA NO to NO₂ through HO₂ and RO₂ are smaller); this may well be compensated by the increased photolysis of East Asian NO₂ to O and decreased chemical losses of East Asian O₃ compared with summertime photochemistry (Table S7).

Based on the fully-tagged approach, we estimate that the acute effects of exposure to East Asian O₃ include 1670 cardiovascular and 300 respiratory premature mortalities in NA in the year 2000 using relative risk values from Bell et al.³ with no threshold for O₃ concentration (Table 1). These deaths are

Table 1. Annual Premature Mortalities (Unit: Deaths) in North America in 2000 Associated with O₃ Originating from EA Emissions Using Sensitivity Analysis, NO_y-Tagging, and Fully Tagged Methods^a

	cardiovascular mortalities	respiratory mortalities
sensitivity analysis	670 (570)	120 (100)
NO _y -tagging method	210 (200)	39 (36)
fully-tagged method	1670 (1542)	300 (275)

^aA threshold of 0 ppbv (and 25 ppbv) O₃ is used.

the most concentrated in the West Coast and eastern U.S., the Caribbean, and Mexico (Figure S10). Assuming a threshold of 25 ppbv slightly decreases the estimates to 1542 cardiovascular and 275 respiratory mortalities in NA. In comparison, NO_y-tagging and sensitivity approaches, respectively, result in a factor of eight and two fewer premature mortalities. Previous sensitivity studies showed that a 20% reduction of East Asian O₃ precursors emissions leads to 200 avoided annual cardiopulmonary mortalities, and a 10% reduction of East Asian O₃ precursor emissions leads to 38 avoided annual mortalities in North America.^{48,49} Scaling up these estimates to 100% emission reduction is comparable to the sensitivity results estimated in this study, although significant nonlinearity of O₃ response to emission perturbation exists.⁵⁷ Our results include

only the acute effects of O₃ exposure. We recognize that chronic O₃ exposure may result in a much larger health burden.⁵⁸

The challenge of meeting increasingly stringent O₃ air quality standards requires accurate attribution of ground-level O₃ to various sources, especially from upwind anthropogenic sources. Previous attempts track the cycling of the nitrogen element within the NO_y family (NO_y-tagging approach) or perturb the source emissions and change the O₃ production efficiency. We have developed, for the first time, a method that fully tags all O₃ precursors and incorporates the impact of CO and VOCs on long-distance transport. The impact of all reactions and reservoir species affecting O₃ concentrations are tracked (e.g., peroxy radicals in addition to reactive nitrogen). This approach accounts for the full contribution of all East Asian anthropogenic pollutants to the formation of O₃ over North America with the state of the atmosphere unchanged. It reveals the importance of long-lived precursors (CO and some hydrocarbons) in driving HO_x-NO_x-RO_x cycling over North America in summer.

Controlling NO_x and reactive VOCs have been the traditional strategies for local O₃ air quality management,^{59,60} yet little attention has been paid to the role of relatively long-lived precursors, such as carbon monoxide and longer-lived VOCs in transboundary transport. In addition to NO_x, large quantities of CO and VOCs are emitted from the industry, residential, and transport sectors in East Asia and were experiencing a rapid increase during 2000–2010,^{16,61} as opposed to a seemingly decrease in NA.^{7,16} Furthermore, from a climate perspective the year 2000 analyzed in this study displayed relatively weak trans-Pacific transport; a La Nina like El Nino Southern Oscillation (ENSO) pattern weakens the storm track and a negative Pacific Decadal Oscillation (PDO) phase weakens the westerlies.⁶² These indicate an even more important role of East Asian emissions in NA O₃ formation for other years. The emissions of CO and VOCs are usually associated with incomplete combustion and low energy-use efficiency,^{17,63} and these processes also co-emit other pollutants (especially black carbon,^{64,65} organic matters, sulfur dioxide, and CO₂). Domestic and international policies that limit emissions and, hence, long-range transport of CO and long-lived VOCs would mitigate the source-receptor attribution of transboundary O₃ while simultaneously reducing black carbon and CO₂, thus achieving multiple co-benefits for global health and climate.

■ ASSOCIATED CONTENT

📄 Supporting Information

This material is free at The Supporting Information is available free of charge on the ACS Publications website at DOI: 10.1021/acs.est.6b05664.

Figures showing the validation of fully-tagged method, the definition of domain size for East Asia and North America, the comparison of different ozone tagging approaches, detailed simulation results, and health damages. Tables showing the comparison of this study to previous works, additional details of the fully-tagged mechanism, the setting of vertical levels, and the ozone budget among different approaches. (PDF)

AUTHOR INFORMATION

Corresponding Author

*Phone and fax: +86 10 6275 7852; e-mail: jfliu@pku.edu.cn.

ORCID

Yixin Guo: 0000-0003-4958-7044

Denise L. Mauzerall: 0000-0003-3479-1798

Shu Tao: 0000-0002-7374-7063

Notes

The authors declare no competing financial interest.

ACKNOWLEDGMENTS

We thank three anonymous reviewers for their thoughtful comments and helpful suggestions. This work was supported by funding from the National Natural Science Foundation of China under award nos. 41671491, 41571130010, and 41390240; National Key Research and Development Program of China 2016YFC0206202; and the 111 Project (B14001); as well as PhD student fellowship support from the Woodrow Wilson School of Public and International Affairs at Princeton University. We also thank the Japan Meteorological Agency for providing observational data through WMO Global Atmosphere Watch (GAW) network.

REFERENCES

- (1) Krzyzanowski, M. Global update of WHO air quality guidelines. *Epidemiology* **2006**, *17* (6), S80–S80.
- (2) Mauzerall, D. L.; Wang, X. Protecting agricultural crops from the effects of tropospheric ozone exposure: reconciling science and standard setting in the United States, Europe, and Asia. *Annu. Rev. Energ. Env.* **2001**, *26* (1), 237–268.
- (3) Bell, M. L.; Dominici, F.; Samet, J. M. A meta-analysis of time-series studies of ozone and mortality with comparison to the national morbidity, mortality, and air pollution study. *Epidemiology (Cambridge, Mass.)* **2005**, *16* (4), 436.
- (4) Giles, J. Hikes in surface ozone could suffocate crops. *Nature* **2005**, *435*, (7), DOI10.1038/435007a.
- (5) Karnosky, D. F.; Pregitzer, K. S.; Zak, D. R.; Kubiske, M. E.; Hendrey, G. R.; Weinstein, D.; Nosal, M.; Percy, K. E. Scaling ozone responses of forest trees to the ecosystem level in a changing climate. *Plant, Cell Environ.* **2005**, *28* (8), 965–981.
- (6) U.S. Environmental Protection Agency. Air quality --- National Summary | National Air Quality: Status and Trends of Key Air Pollutants; <https://www.epa.gov/air-trends/air-quality-national-summary>, 2015 (accessed Jan 28, 2017).
- (7) U.S. Environmental Protection Agency. National Emissions Inventory (NEI) Air Pollutant Emissions Trends Data; <https://www.epa.gov/air-emissions-inventories/air-pollutant-emissions-trends-data>, 2016 (accessed Jan 28, 2017).
- (8) Fiore, A. M.; Oberman, J. T.; Lin, M. Y.; Zhang, L.; Clifton, O. E.; Jacob, D. J.; Naik, V.; Horowitz, L. W.; Pinto, J. P.; Milly, G. P. Estimating North American background ozone in U.S. surface air with two independent global models: Variability, uncertainties, and recommendations. *Atmos. Environ.* **2014**, *96*, 284–300.
- (9) Lin, M.; Fiore, A. M.; Cooper, O. R.; Horowitz, L. W.; Langford, A. O.; Levy, H.; Johnson, B. J.; Naik, V.; Oltmans, S. J.; Senff, C. J. Springtime high surface ozone events over the western United States: Quantifying the role of stratospheric intrusions. *J. Geophys. Res., [Atmos.]* **2012**, *117*, D21; 10.1029/2012JD018151.
- (10) Trainer, M.; Williams, E. J.; Parrish, D.; Buhr, M.; Allwine, E.; Westberg, H.; Fehsenfeld, F. C.; Liu, S. C. Models and observations of the impact of natural hydrocarbons on rural ozone. *Nature* **1987**, *329*, 705–707.
- (11) Fiore, A. M.; Pierce, R. B.; Dickerson, R. R.; Lin, M.; Bradley, R. Detecting and attributing episodic high background ozone events. *J. Air Waste Manage. Assoc.* **2014**, *64*, 22.
- (12) Lin, M.; Fiore, A. M.; Horowitz, L. W.; Cooper, O. R.; Naik, V.; Holloway, J.; Johnson, B. J.; Middlebrook, A. M.; Oltmans, S. J.; Pollack, I. B. Transport of Asian ozone pollution into surface air over the western United States in spring. *J. Geophys. Res., [Atmos.]* **2012**, *117* (D21); 10.1029/2011JD016961.
- (13) Zhang, L.; Jacob, D. J.; Boersma, K. F.; Jaffe, D. A.; Olson, J. R.; Bowman, K. W.; Worden, J. R.; Thompson, A. M.; Avery, M. A.; Cohen, R. C.; Dibb, J. E.; Flock, F. M.; Fuelberg, H. E.; Huey, L. G.; McMillan, W. W.; Singh, H. B.; Weinheimer, A. J. Transpacific transport of ozone pollution and the effect of recent Asian emission increases on air quality in North America: an integrated analysis using satellite, aircraft, ozonesonde, and surface observations. *Atmos. Chem. Phys.* **2008**, *8* (20), 6117–6136.
- (14) Verstraeten, W. W.; Neu, J. L.; Williams, J. E.; Bowman, K. W.; Worden, J. R.; Boersma, K. F. Rapid increases in tropospheric ozone production and export from China. *Nat. Geosci.* **2015**, *8* (9), 690–695.
- (15) Lamsal, L.; Martin, R.; Padmanabhan, A.; van Donkelaar, A.; Zhang, Q.; Sioris, C.; Chance, K.; Kurosu, T.; Newchurch, M. Application of satellite observations for timely updates to global anthropogenic NOx emission inventories. *Geophys. Res. Lett.* **2011**, *38*, (5); 10.1029/2010GL046476.
- (16) Granier, C.; Bessagnet, B.; Bond, T.; D'Angiola, A.; van Der Gon, H. D.; Frost, G. J.; Heil, A.; Kaiser, J. W.; Kinne, S.; Klimont, Z. Evolution of anthropogenic and biomass burning emissions of air pollutants at global and regional scales during the 1980–2010 period. *Clim. Change* **2011**, *109* (1–2), 163.
- (17) Zhang, Q.; Streets, D. G.; Carmichael, G. R.; He, K.; Huo, H.; Kannari, A.; Klimont, Z.; Park, I.; Reddy, S.; Fu, J.; et al. Asian emissions in 2006 for the NASA INTEX-B mission. *Atmos. Chem. Phys.* **2009**, *9* (14), 5131–5153.
- (18) Finlayson-Pitts, B. J.; Pitts, J. N. Tropospheric air pollution: ozone, airborne toxics, polycyclic aromatic hydrocarbons, and particles. *Science* **1997**, *276* (5315), 1045–1051.
- (19) Myhre, G.; Shindell, D.; F.-M., Bréon; Collins, W.; Fuglestedt, J.; Huang, J.; Koch, D.; Lamarque, J.-F.; Lee, D.; Mendoza, B.; Nakajima, T.; Robock, A.; Stephens, G.; Takemura, T.; Zhang, H. Anthropogenic and Natural Radiative Forcing. In: *Climate Change 2013: The Physical Science Basis. Contribution of Working Group I to the Fifth Assessment Report of the Intergovernmental Panel on Climate Change*; Stocker, T. F., Qin, D., Plattner, G.-K.; Tignor, M.; Allen, S.K.; Boschung, J.; Nauels, A.; Xia, Y.; Bex, V.; Midgley, P.M., Eds.; Cambridge University Press: Cambridge, United Kingdom, 2013, pp 659–740; 10.1017/CBO9781107415324.018
- (20) Sitoh, S.; Cox, P.; Collins, W.; Huntingford, C. Indirect radiative forcing of climate change through ozone effects on the land-carbon sink. *Nature* **2007**, *448* (7155), 791–794.
- (21) Unger, N.; Shindell, D. T.; Koch, D. M.; Streets, D. G. Cross influences of ozone and sulfate precursor emissions changes on air quality and climate. *Proc. Natl. Acad. Sci. U. S. A.* **2006**, *103* (12), 4377–4380.
- (22) Jacob, D. J.; Logan, J. A.; Murti, P. P. Effect of rising Asian emissions on surface ozone in the United States. *Geophys. Res. Lett.* **1999**, *26* (14), 2175–2178.
- (23) Wild, O.; Akimoto, H. Intercontinental transport of ozone and its precursors in a three-dimensional global CTM. *J. Geophys. Res., [Atmos.]* **2001**, *106* (D21), 27729–27744.
- (24) Fiore, A. M. Background ozone over the United States in summer: Origin, trend, and contribution to pollution episodes. *J. Geophys. Res.* **2002**, *107*, (D15); 10.1029/2001JD000982.
- (25) Fiore, A. M.; Dentener, F. J.; Wild, O.; Cuvelier, C.; Schultz, M. G.; Hess, P.; Textor, C.; Schulz, M.; Doherty, R. M.; Horowitz, L. W.; MacKenzie, I. A.; Sanderson, M. G.; Shindell, D. T.; Stevenson, D. S.; Szopa, S.; Van Dingenen, R.; Zeng, G.; Atherton, C.; Bergmann, D.; Bey, I.; Carmichael, G.; Collins, W. J.; Duncan, B. N.; Faluvegi, G.; Folberth, G.; Gauss, M.; Gong, S.; Hauglustaine, D.; Holloway, T.; Isaksen, I. S. A.; Jacob, D. J.; Jonson, J. E.; Kaminski, J. W.; Keating, T. J.; Lupu, A.; Marmor, E.; Montanaro, V.; Park, R. J.; Pitari, G.; Pringle, K. J.; Pyle, J. A.; Schroeder, S.; Vivanco, M. G.; Wind, P.; Wojcik, G.; Wu, S.; Zuber, A. Multimodel estimates of intercontinental source-

receptor relationships for ozone pollution. *J. Geophys. Res.* **2009**, *114*; 10.1029/2008JD010816.

(26) Dentener, F.; Keating, T.; Akimoto, H. *HTAP (hemispheric transport of air pollution)(2010): part A: ozone and particulate matter air pollution studies Nr. 17*; United Nations Publication: New York, 2011.

(27) Simon, H.; Reff, A.; Wells, B.; Xing, J.; Frank, N. Ozone trends across the United States over a period of decreasing NO_x and VOC emissions. *Environ. Sci. Technol.* **2015**, *49* (1), 186–195.

(28) Bey, I.; Jacob, D. J.; Logan, J. A.; Yantosca, R. M. Asian chemical outflow to the Pacific in spring: Origins, pathways, and budgets. *J. Geophys. Res.* **2001**, *106* (D19), 23097–23113.

(29) Sudo, K.; Akimoto, H. Global source attribution of tropospheric ozone: Long-range transport from various source regions. *J. Geophys. Res.* **2007**, *112*, (D12); 10.1029/2006JD007992.

(30) Wang, P.-H.; Cunnold, D. M.; Zawodny, J. M.; Pierce, R. B.; Olson, J. R.; Kent, G. S.; Skeens, K. M. Seasonal ozone variations in the isentropic layer between 330 and 380 K as observed by SAGE II: Implications of extratropical cross-tropopause transport. *J. Geophys. Res., [Atmos.]* **1998**, *103* (D22), 28647–28659.

(31) Horowitz, L. W.; Liang, J. Y.; Gardner, G. M.; Jacob, D. J. Export of reactive nitrogen from North America during summertime: Sensitivity to hydrocarbon chemistry. *J. Geophys. Res., [Atmos.]* **1998**, *103* (D11), 13451–13476.

(32) Derwent, R. G.; Utembe, S. R.; Jenkin, M. E.; Shallcross, D. E. Tropospheric ozone production regions and the intercontinental origins of surface ozone over Europe. *Atmos. Environ.* **2015**, *112*, 216–224.

(33) Ying, Q.; Krishnan, A. Source contributions of volatile organic compounds to ozone formation in southeast Texas. *J. Geophys. Res.* **2010**, *115*, (D17); 10.1029/2010JD013931.

(34) Emmons, L. K.; Hess, P. G.; Lamarque, J. F.; Pfister, G. G. Tagged ozone mechanism for MOZART-4, CAM-chem and other chemical transport models. *Geosci. Model Dev.* **2012**, *5* (6), 1531–1542.

(35) Brown-Steiner, B.; Hess, P. Asian influence on surface ozone in the United States: A comparison of chemistry, seasonality, and transport mechanisms. *J. Geophys. Res.* **2011**, *116*; 10.1029/2011JD015846.

(36) Kwok, R.; Baker, K.; Napelenok, S.; Tonnesen, G. Photochemical grid model implementation and application of VOC, NO_x, and O₃ source apportionment. *Geosci. Model Dev.* **2015**, *8* (1), 99–114.

(37) ENVIRON International Corporation. User's Guide—Comprehensive Air Quality Model with Extensions, version 4.50; ENVIRON: Novato, CA, 2008.

(38) Seinfeld, J. H.; Pandis, S. N.; Noone, K. *Atmospheric Chemistry and Physics: From Air Pollution to Climate Change*; American Institute of Physics: College Park, MD, 1998.

(39) Emmons, L.; Walters, S.; Hess, P.; Lamarque, J.-F.; Pfister, G.; Fillmore, D.; Granier, C.; Guenther, A.; Kinnison, D.; Laepple, T.; et al. Description and evaluation of the Model for Ozone and Related chemical Tracers, version 4 (MOZART-4). *Geosci. Model Dev.* **2010**, *3* (1), 43–67.

(40) Emmons, L. K.; Hauglustaine, D. A.; Müller, J.-F.; Carroll, M. A.; Brasseur, G. P.; Brunner, D.; Staehelin, J.; Thouret, V.; Marenco, A. Data composites of airborne observations of tropospheric ozone and its precursors. *J. Geophys. Res., [Atmos.]* **2000**, *105* (D16), 20497–20538.

(41) Granier, C.; Lamarque, J. F.; Mieville, A.; Müller, J. F.; Olivier, J.; Orlando, J.; Peters, J.; Petron, G.; Tyndall, G.; Wallens, S. POET, a database of surface emissions of ozone precursors. <http://www.aero.jussieu.fr/projet/ACCENT/POET.php> (accessed Apr 2, 2016).

(42) Guenther, A.; Karl, T.; Harley, P.; Wiedinmyer, C.; Palmer, P. I.; Geron, C. Estimates of global terrestrial isoprene emissions using MEGAN (Model of Emissions of Gases and Aerosols from Nature). *Atmos. Chem. Phys.* **2006**, *6* (11), 3181–3210.

(43) EANET. *Data Report on the Acid Deposition in the East Asian Region*. Summary of the Second Intergovernmental Meeting on the

Acid Deposition monitoring Network in East Asia; EANET: Niigata, Japan, 2000.

(44) Lin, M.; Holloway, T.; Carmichael, G. R.; Fiore, A. M. Quantifying pollution inflow and outflow over East Asia in spring with regional and global models. *Atmos. Chem. Phys.* **2010**, *10*, (9); 4221423910.5194/acp-10-4221-2010.

(45) Li, X.; Liu, J.; Mauzerall, D. L.; Emmons, L. K.; Walters, S.; Horowitz, L. W.; Tao, S. Effects of trans-Eurasian transport of air pollutants on surface ozone concentrations over Western China. *J. Geophys. Res., [Atmos.]* **2014**, *119* (21), 12338–12354.

(46) Appel, K. W.; Gilliland, A. B.; Sarwar, G.; Gilliam, R. C. Evaluation of the Community Multiscale Air Quality (CMAQ) model version 4.5: sensitivities impacting model performance: part I—ozone. *Atmos. Environ.* **2007**, *41* (40), 9603–9615.

(47) Possiel, N.; Stella, G.; Ryan, R.; Pace, T.; Benjey, W.; Beidler, A.; Kinnee, E.; Houyoux, M.; Adelman, Z. *Development of an Anthropogenic Emissions Inventory for Annual Nationwide Models-3/Cmaq Simulations of Ozone and Aerosols*; Proceedings of the International Emission Inventory Conference; Environmental Protection Agency: Denver, CO, 2001.

(48) West, J. J.; Naik, V.; Horowitz, L. W.; Fiore, A. M. Effect of regional precursor emission controls on long-range ozone transport - Part 2: Steady-state changes in ozone air quality and impacts on human mortality. *Atmos. Chem. Phys.* **2009**, *9* (16), 6095–6107.

(49) Anenberg, S. C.; West, J. J.; Fiore, A. M.; Jaffe, D. A.; Prather, M. J.; Bergmann, D.; Cuvelier, K.; Dentener, F. J.; Duncan, B. N.; Gauss, M.; Hess, P.; Jonson, J. E.; Lupu, A.; MacKenzie, I. A.; Marmor, E.; Park, R. J.; Sanderson, M. G.; Schultz, M.; Shindell, D. T.; Szopa, S.; Vivanco, M. G.; Wild, O.; Zeng, G. Intercontinental Impacts of Ozone Pollution on Human Mortality. *Environ. Sci. Technol.* **2009**, *43* (17), 6482–6487.

(50) National Center for Health Statistics, Centers for Disease Control and Prevention (2008-10-18). Deaths by Age (1999 to 2004) [Archive]: Deaths - Age Not Specified | Cause of Death: All Causes of Death | Gender: All Genders, 2004. Data-Planet Statistical Datasets by Conquest Systems, Inc. [Data-file]. Dataset-ID: 005-011-002 (accessed Aug 9, 2016).

(51) CIESIN. Gridded Population of the World (GPW), version 3. CIESIN: Palisades, NY, 2005.

(52) Cai, C.; Geng, F.; Tie, X.; Yu, Q.; An, J. Characteristics and source apportionment of VOCs measured in Shanghai, China. *Atmos. Environ.* **2010**, *44* (38), 5005–5014.

(53) Brasseur, G.; Orlando, J. J.; Tyndall, G. S. *Atmospheric chemistry and global change*; Oxford University Press: New York, NY, 1999.

(54) Cooper, O.; Oltmans, S.; Johnson, B.; Brioude, J.; Angevine, W.; Trainer, M.; Parrish, D.; Ryerson, T.; Pollack, I.; Cullis, P. et al. Measurement of western US baseline ozone from the surface to the tropopause and assessment of downwind impact regions. *J. Geophys. Res., [Atmos.]* **2011**, *116* (D21); DOI10.1029/2011JD016095.

(55) Cooper, O. R.; Parrish, D. D.; Stohl, A.; Trainer, M.; Nedelec, P.; Thouret, V.; Cammas, J. P.; Oltmans, S. J.; Johnson, B. J.; Tarasick, D.; Leblanc, T.; McDermid, I. S.; Jaffe, D.; Gao, R.; Stith, J.; Ryerson, T.; Aikin, K.; Campos, T.; Weinheimer, A.; Avery, M. A. Increasing springtime ozone mixing ratios in the free troposphere over western North America. *Nature* **2010**, *463* (7279), 344–348.

(56) Lin, M. Y.; Horowitz, L. W.; Cooper, O. R.; Tarasick, D.; Conley, S.; Iraci, L. T.; Johnson, B.; Leblanc, T.; Petropavlovskikh, I.; Yates, E. L. Revisiting the evidence of increasing springtime ozone mixing ratios in the free troposphere over western North America. *Geophys. Res. Lett.* **2015**, *42* (20), 8719–8728.

(57) Wu, S.; Duncan, B. N.; Jacob, D. J.; Fiore, A. M.; Wild, O. Chemical nonlinearities in relating intercontinental ozone pollution to anthropogenic emissions. *Geophys. Res. Lett.* **2009**, *36*, (5); 10.1029/2008GL036607.

(58) Jerrett, M.; Burnett, R. T.; Pope, C. A., III; Ito, K.; Thurston, G.; Krewski, D.; Shi, Y.; Calle, E.; Thun, M. Long-term ozone exposure and mortality. *N. Engl. J. Med.* **2009**, *360* (11), 1085–1095.

(59) EPA. Control Techniques Guidelines and Alternative Control Techniques Documents for Reducing Ozone-Causing Emissions.

<https://www.epa.gov/ozone-pollution/control-techniques-guidelines-and-alternative-control-techniques-documents-reducing> (accessed Mar 21, 2017).

(60) EPA. Evaluating ozone control programs in the eastern United States: Focus on the NO_x budget trading program. EPA Report EPA454-K-05-001; EPA: Washington, D.C., 2005.

(61) Dentener, F.; Stevenson, D.; Cofala, J.; Mechler, R.; Amann, M.; Bergamaschi, P.; Raes, F.; Derwent, R. The impact of air pollutant and methane emission controls on tropospheric ozone and radiative forcing: CTM calculations for the period 1990–2030. *Atmos. Chem. Phys.* **2005**, *5* (7), 1731–1755.

(62) Lin, M.; Horowitz, L. W.; Oltmans, S. J.; Fiore, A. M.; Fan, S. Tropospheric ozone trends at Mauna Loa Observatory tied to decadal climate variability. *Nat. Geosci.* **2014**, *7* (2), 136–143.

(63) Bond, T. C.; Streets, D. G.; Yarber, K. F.; Nelson, S. M.; Woo, J. H.; Klimont, Z. A technology-based global inventory of black and organic carbon emissions from combustion. *J. Geophys. Res.* **2004**, *109*, (D14); [10.1029/2003JD003697](https://doi.org/10.1029/2003JD003697).

(64) Miguel, A. H.; Kirchstetter, T. W.; Harley, R. A.; Hering, S. V. On-road emissions of particulate polycyclic aromatic hydrocarbons and black carbon from gasoline and diesel vehicles. *Environ. Sci. Technol.* **1998**, *32* (4), 450–455.

(65) Kondo, Y.; Komazaki, Y.; Miyazaki, Y.; Moteki, N.; Takegawa, N.; Kodama, D.; Deguchi, S.; Nogami, M.; Fukuda, M.; Miyakawa, T. et al. Temporal variations of elemental carbon in Tokyo. *J. Geophys. Res.* **2006**, *111*, (D12); [10.1029/2005JD006257](https://doi.org/10.1029/2005JD006257).